25th ABCM International Congress of Mechanical Engineering
October 20-25, 2019, Uberlândia, MG, Brazil

ANALYSIS OF THE DYNAMIC BEHAVIOR OF A COMPOSITE HOLLOW SHAFT CONSIDERING UNCERTAIN AND SENSITIVITY INFORMATION

Leandro Soares Silva
Paulo C. P. de F. Barbosa
Aldemir Ap. Cavalini Jr
Valder Steffen Jr
LMEst - Structural Mechanics Laboratory, Federal University of Uberlândia, School of Mechanical Engineering, Uberlândia, MG, Brazil, leandrosoares@ufu.br

Fabian Andres Lara-Molina
Federal University of Technology - Paraná, Mechanical Engineering Department, Cornélio Procópio, PR, Brazil.

Abstract. *Composite materials have been widely used in engineering applications due to their advantages over conventional materials. Following this trend, researchers on rotordynamics have shown interest in the substitution of metallic shafts by composite shafts, resulting in higher operating speeds, improvements of the efficiency, and weight decreasing, among other potential advantages. In this contribution, the so-called Simplified Homogenized Beam Theory (SHBT) associated with the finite element (FE) method was used to model a rotating machine composed of a composite shaft. The formulated model was used to represent the dynamic behavior of the rotor operating under sub-critical conditions. The definition of several parameters of the composite shaft is required for the corresponding numerical model. Nevertheless, small variations on these parameters can modify the dynamic behavior of the shaft. Thus, interval uncertainty and sensitivity analyses are used to assess the vibration responses of the composite shaft. The effects of the uncertain parameters on the dynamic behavior of the rotor system are evaluated for different rotation speeds.*

Keywords: *rotating machine, composite hollow shaft, uncertainty analysis, interval approach, sensitivity analysis.*

1. INTRODUCTION

Composite materials are those composed of two or more materials in order to obtain a different one with better characteristics, taking the best advantage of each material. The use of composite materials has been growing over the years, mainly in maritime, aeronautical, and automotive industries since they allow for obtaining required characteristics that are suitable for different application. In this context, shafts of rotating machines can benefit from the use of composite materials (Kuschmierz *et al.*, 2015).

For rotating machines operating under subcritical conditions (rigid rotors), the low weight of composite shafts permits faster acceleration and deceleration (Brush, 1999). Regarding supercritical operations (flexible rotors), where the vibrations associated with shaft bending, dynamic stresses, stability issues, and fatigue are significant, the techniques of manufacturing rotor components in composite materials allow for the customization of mechanical properties (Lees, 2011). This can be performed through changes in the shaft design, such as the number of layers and the orientation of the fibers, thus modifying the critical speeds of the rotating machine, in accordance with the required operation range of the equipment (Gupta, 2015). Thus, composite shafts appears as a viable solution to minimize problems inherent to metallic shafts.

Different methodologies have been proposed in the literature aiming at modeling the dynamic behavior of composite materials. Sino (2007) proposed the SHBT (Simplified Homogenized Beam Theory) equivalent beam model, in which the internal damping of the material is taken into account. This model is based on the direct homogenization of the stiffness and internal damping of the shaft. In this case, the internal damping was developed by using the Kelvin-Voigt rheological model. Sino (2007) demonstrated that this method can be used for symmetric and asymmetric stacking sequences.

Uncertain and sensitivity analysis in rotating machines has been studied in previous contributions to evaluate the behavior of the system as a function of the variation of mechanical and geometric properties. Koroishi *et al.* (2018) analyzed a smart flexible rotor under random uncertainties parameters. Molina *et al.* (2019) proposed a novel alternative to analyze the effect of uncertain interval parameters on the dynamic responses of a flexible rotor by using an interval based methodology.

It is well known that small variations on the parameters can modify the dynamic behavior of composite materials. Thus, in this work, an interval uncertainty analysis (Moore *et al.*, 2009) is performed in a composite hollow shaft with

two discs and supported by two self-alignment ball bearings. A sensitivity analysis (Moens and Vandepitte, 2006, 2007) is also performed to evaluate the effects of the uncertain parameters on the dynamic behavior of the shaft for five different rotation speeds. The SHBT approach associated with the Timoshenko beam theory is used to obtain the FE model of the composite shaft. The physical parameters of the shaft and the positions of the rotating machine' components are considered as uncertain information.

2. ROTOR MODELING

Equation (1) is the differential equation that represents the dynamic behavior of flexible rotors considering the effects associated with composite materials (Sino, 2007).

$$[M]\{\ddot{\delta}\} + [D + \Omega D_g + D_i]\{\dot{\delta}\} + [K + \Omega K_i]\{\delta\} = W + F_u \tag{1}$$

where M is the mass matrix, D is the damping matrix associated with the bearings, D_g represents the gyroscopic effect, and K is the stiffness matrix. D_i and K_i are the internal damping and the stiffness matrix, respectively, associated with the composite material. The vector δ is the generalized coordinates (i.e., lateral vibrations of the shaft) and Ω is the rotation speed of the shaft. W represents the weight of rotating parts and F_u are the unbalance forces.

3. SHBT APPROACH

The homogenization method SHBT was used to obtain the equivalent elastic properties of the shaft. These parameters are used to obtain the internal damping matrix D_i and internal stiffness matrix K_i. Figure 1 shows the schematic representation of the fibers direction in a ply of a given composite material. The Cartesian system follows the inertial directions (X,Y,Z) adopted for the composite shaft. Axes 1, 2, and 3 are associated with the fibers directions, the direction transverse to the fibers, and the direction perpendicular to the ply, respectively. The angle $\theta_{\mathbf{p}}$ represents the orientation of the fibers in each ply.

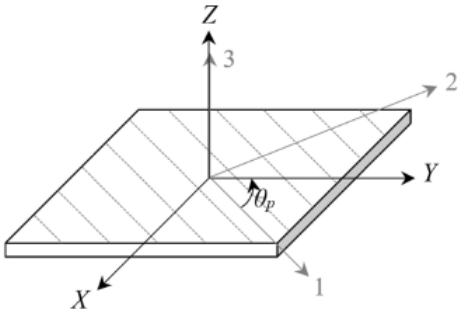

Figure 1. Schematic representation of the fibers direction of the composite shaft (Cavalini Jr. *et al.*, 2016).

The composite material can be characterized by 5 independent elastic constants, namely E_1, E_2 (Young's modulus), G_{12} (shear modulus), υ_{12} and υ_{21} (Poisson's coefficient). In this case, a transversely isotropic material is considered. Assuming that the plies of the composite shaft are thin, the stiffness matrix representing its mechanical characteristics is given by Eq. (2).

$$Q = \begin{vmatrix} \frac{E_1}{1-\nu_{12}\nu_{21}} & \frac{E_2\nu_{12}}{1-\nu_{12}\nu_{21}} & 0 \\ \frac{E_1\nu_{21}}{1-\nu_{12}\nu_{21}} & \frac{E_2}{1-\nu_{12}\nu_{21}} & 0 \\ 0 & 0 & G_{12} \end{vmatrix} = \begin{vmatrix} Q_{11} & Q_{12} & 0 \\ Q_{21} & Q_{22} & 0 \\ 0 & 0 & Q_{66} \end{vmatrix} \tag{2}$$

Thus, the SHBT approach is applied to obtain equivalent values for the elastic properties of the shaft. These parameters are used to determine the FE matrices K, D_i, and K_i, as shown in Eq. (1). The effect of the internal damping is included in the matrices D_i and K_i. These matrices are associated with the FE model of the composite shaft. Details about the formulation of the elementary FE matrices are given in Sino (2007).

The SHBT approach is based on the direct homogenization of the product EI_{eq}, GS_{eq}, and $EI_{eq\alpha}$, namely equivalent stiffness, equivalent shear stiffness, and equivalent damping, respectively. In addition, it takes into account the distance of each layer to the neutral axis of the shaft. The equivalent stiffness of the shaft in bending is given by Eq. (3).

$$EI_{eq} = \sum_{p=1}^{N} E_y^p I^p \qquad I^p = \pi \frac{(R_p^4 - R_{p-1}^4)}{4} \tag{3}$$

where E_y^p is the Young's modulus of the ply p, as given by Eq. (4), and I^p is the inertia moment of the ply cross-sectional area. R_{p-1} and R_p are the inner and outer radius of the ply p, respectively.

$$E_y^p = \left[\frac{cos^4(\theta_p)}{E_1} + \frac{sin^4(\theta_p)}{E_2} + cos^2(\theta_p) sin^2(\theta_p) \left(\frac{1}{G_{12}} - 2\frac{\upsilon_{12}}{E_1} \right) \right]^{-1} \tag{4}$$

The equivalent shear stiffness is presented in Eq. (5).

$$GS_{eq} = \sum_{p=1}^{N} G_{12}^p S^p \qquad S^p = \pi(R_p^2 - R_{p-1}^2) \tag{5}$$

where G_{12}^p is the shear modulus of the ply p, as given by Eq.(6), and S^p is the cross-section area of the ply p.

$$G_{12}^p = \left[2sin^2\theta cos^2\theta \left(\frac{2}{E_1} + \frac{2}{E_2} + \frac{4\upsilon_{12}}{E_1} - \frac{1}{G_{12}} \right) + \frac{sin^4\theta cos^4\theta}{G_{12}} \right]^{-1} \tag{6}$$

The equivalent damping associated with the stiffness and the shear stiffness ($EI_{eq\alpha}$ and $GS_{eq\alpha}$, respectively) are given by Eq. (7).

$$EI_{eq\alpha} = \sum_{p=1}^{N} E_{y\alpha}^p I^p \qquad GS_{eq\alpha} = \sum_{p=1}^{N} G_{12\alpha}^p S^p \tag{7}$$

in which $E_{y\alpha}^p$ and $G_{12\alpha}^p$ are obtained by using the stiffness matrix associated with the damping factors $\psi_{\mathbf{11}}$ and $\psi_{\mathbf{12}}$.

4. UNCERTAINTY ANALYSIS

The interval problem related to the uncertainty analysis consists in computing the variation of the numerical model responses with respect to the considered uncertain parameters (Modares and Mullen, 2013). The mathematical model of a dynamic system $\mathbf{M}$ that expresses the relationship between the outputs $\mathbf{y}$ (responses) and the input is defined by the set of differential equations $\mathbf{f}$ as presented in Eq. (8).

$$M : y = \mathbf{f}(\mathbf{p}, \tau) \tag{8}$$

where the inputs of the model are the set of parameters $\mathbf{p}$ and an independent variable of the dynamic response τ that may represent the time, frequency, or spatial coordinates. The primary objective of the uncertain interval analysis is to compute the variation of the outputs $\bar{\mathbf{y}}$, which is obtained from $\mathbf{M}$ by considering that $\mathbf{p}$ can vary between the lower and upper limits $\mathbf{p_l}$ and $\mathbf{p_u}$, respectively. Consequently:

$$\bar{y} = \bar{\mathbf{f}}(\bar{\mathbf{p}}, \tau) \tag{9}$$

where $\mathbf{p} = [\mathbf{p_l}, \mathbf{p_u}]$ and $\mathbf{y} = [\mathbf{y_l}, \mathbf{y_u}]$. $\bar{\mathbf{f}}$ is an interval function that represents the relationship between the input and output intervals.

The global optimization method is used in this contribution. The output interval is determined by the maximization and minimization of the objective function $\mathbf{f}$ in the domain $\bar{\mathbf{p}}$ that corresponds to the definition of the uncertain parameters. Thus, the optimization problems associated with the global optimization strategy are expressed as follows:

$$y_l(\tau) = \min_{\mathbf{p}\epsilon\bar{\mathbf{p}}} f(\mathbf{p},\tau) \qquad y_r(\tau) = \max_{\mathbf{p}\epsilon\bar{\mathbf{p}}} f(\mathbf{p},\tau) \tag{10}$$

This strategy permits to find the upper and lower limits of the uncertain interval, which correspond to the variation of the output produced by the uncertain parameters. In this case, the Differential Evolution algorithm (Storn and Price, 1997) was used to maximize and minimize the objective function, which is the maximum vibration amplitude.

5. INTERVAL SENSITIVITY ANALYSIS

The objective of sensitivity analysis is to quantify the individual contribution of each uncertain interval parameter on the uncertain interval responses as obtained by using the numerical model of the system (Moens and Vandepitte, 2006). The numerical procedure used to compute the interval sensitivity analysis is presented next. The relationship between the interval input and the interval output is defined as the function f^{Δ}, which relates the input interval radius to the output interval radius. The interval radius is determined as shown by Eq. (11).

$$\Delta y = \frac{y_l - y_u}{2} \tag{11}$$

Consequently, the relationship between the interval input and the interval output is expressed as follows:

$$\Delta y = f^{\Delta}(\Delta p) \tag{12}$$

The interval function f^{Δ} is used to define the absolute sensitivity of the interval output $\bar{y}$ with respect to the interval input $\bar{p}$ as given by Eq.(13) . In this case, the interval sensitivity is obtained by the relationship between the widths of $\bar{y}$ and $\bar{p}$.

$$\delta_{\bar{p}_i}^{\bar{y}} = \frac{\partial(\Delta y)}{\partial(\Delta p)} = \frac{\partial f(\Delta p)}{\partial(\Delta p)} \tag{13}$$

The output interval depends on multiple intervals when various uncertain parameters are considered simultaneously. The relationship between the interval widths of $\bar{y}$ and $\bar{p}$ provides a perception on the interval sensitivity. Therefore, Eq. (14) defines the relative interval sensitivity.

$$\rho_{\bar{p}}^{\bar{y}} = \frac{\partial(\frac{\Delta y_i}{\Delta y_i^*})}{\partial(\frac{\Delta p_i}{\Delta p_i^*})} = \frac{\Delta p_i^*}{\Delta y_i^*} \times \delta_{\bar{p}_i}^{\bar{y}} \tag{14}$$

where $\Delta y_i^* = y_{ui} - y_{li}$ and $\Delta p_i^* = p_{ui} - p_{li}$ are the nominal interval widths obtained by solving Eq. (15) for each uncertain parameter, separately.

$$y_{li}(\tau) = \min_{p_{li}\epsilon\bar{p}_i} f(p_{li},\tau) \qquad y_{ui}(\tau) = \max_{p_{ui}\epsilon\bar{p}_i} f(p_{ui},\tau) \tag{15}$$

The interval sensitivity represents the variation of the output interval concerning changes in the input interval. Dimensionless interval sensitivities for each uncertain parameter are obtained. Thus, the influence of the interval uncertainties can be determined by considering different operational scenarios of the analyzed system. The normalized interval sensitivity is defined by Eq. (16), which represents the importance of the total interval sensitivity of the system subjected to the interval uncertainties.

$$\upsilon_{\bar{p}_i}^{\bar{y}} = \frac{\rho_{\bar{p}_i}^{\bar{y}}}{\sum_{i=1}^{n} \rho_{\bar{p}_i}^{\bar{y}}} \tag{16}$$

The definition of the normalized relative interval sensitivity permits an objective comparison regarding the influence of the individual inputs on the model output. This an important contribution in the context of the analysis of flexible structures, which deals with structures discretized using the FE method along with uncertain parameters modeled as intervals. Moreover, Eq. (14) and Eq. (16) show the relative sensitivity and the normalized sensitivity that can be computed based on the absolute interval sensitivity of Eq. (13).

The interval function (see Eq. (12)) can be computed based on the definition of the absolute interval sensitivity. However, the absolute interval uncertainty is obtained based on the definition of the interval radius as described in Eq. (11). Thus, Eq. (17) is computed based on the upper and lower limits $\delta_{\bar{p}}^{\bar{y}_l}$ and $\delta_{\bar{p}}^{\bar{y}_u}$, respectively:

$$\delta_{\bar{p}_i}^{\bar{y}} = \frac{\partial \Delta y}{\partial \Delta p} = \frac{1}{2}\left(\frac{\partial y_l}{\partial \Delta p} - \frac{\partial y_u}{\partial \Delta p}\right) = \frac{1}{2}(\delta_{\bar{p}}^{y_l} - \delta_{\bar{p}}^{y_u}) \tag{17}$$

which represents how the upper and lower limits change according to variations introduced in the input interval parameters. As mentioned, the global optimization strategy was used to obtain the upper and lower limits of Eq. (17). The upper and lower sensitivities express the variation on the upper and lower limits (y_u and y_l, respectively) obtained from the interval analysis. This variation is computed based on Δp, which is the variation of the radius associated with the input interval parameter. In this procedure the following points should be taken into account:

The change of the upper and lower bounds obeys the following expressions:

$$\delta_{\bar{p}_i}^{y_l} = \frac{\partial y_l}{\partial \Delta p} \leq 0 \qquad\qquad \delta_{\bar{p}_i}^{y_u} = \frac{\partial y_u}{\partial \Delta p} \geq 0 \tag{18}$$

The sensitivity of the limits is not zero only if y_r and y_l correspond to the local optimal points of the function f within the interval $\bar{p}$.

Consequently, the upper and lower sensitivity limits are related to the behavior of the function f regarding the evaluation of p^{y_l} and p^{y_u} . The upper and lower limits of the sensitivity are computed by using Eq. (19).

$$\delta_{\bar{p}_i}^{y_l} = -\left|\left(\frac{\partial y}{\partial p}\right)_{p^{y_l}}\right| \qquad\qquad \delta_{\bar{p}_i}^{y_u} = \left|\left(\frac{\partial y}{\partial p}\right)_{p^{y_u}}\right| \tag{19}$$

which indicates that for the interval outputs obtained using the global optimization method, the sensitivity limits will correspond to the gradients at the end of the optimization process. Finally, the absolute interval sensitivity is obtained by applying Eq. (17).

6. NUMERICAL RESULTS

Figure (2) shows the experimental test rig used as a reference in the present contribution. It is a horizontal rotating system (SpectraQuest model MFS-RDS) fixed on an inertia base. The experimental setup is composed by two discs, two self-alignment ball bearings and a composite hollow shaft. Two sensors are located in the same position of the discs. The coupling between the AC motor and the shaft is a Rocom® flexible anodized aluminum coupling. The composite hollow shaft is made of special high-modulus pre-impregnated carbon fiber plies, presenting twenty layers with the following stacking sequence: [0, 0, 0, 0, 90, 90, 45,-45, 0, 0, 0, 45,-45, 90, 90, 0, 0, 0, 0, 0/90] (degrees of inclination, relative to the Y direction as given in Fig. 1), from the most internal to the most external ply. The last layer is made of a crossed mesh with interspersed filaments of carbon fibers, where half the fibers are at 0 and half at 90 degrees. The shaft has 907 mm length, 18 mm outer diameter, 12.8 mm inner diameter, and $1677 Kg/m^3$ density. The discs and the bearings have 0.656 Kg and 0.205 Kg mass each, respectively.

The effects of the uncertain parameters on the vibration amplitudes of the composite shaft is presented next. In this case, different rotation speeds are considered for the rotor. Table (1) shows the uncertain scenario evaluated in the numerical simulations. Variations of $\pm 5\%$ around the nominal values of the shaft material properties are considered. However, ± 1 degree and ± 1 mm are applied in the orientation of the fibers and the positions of the discs and bearings, respectively.

Figure (3) shows the maximum vibration amplitude (sensors 1 and 2) of the rotor operating at 300, 600, 900, 1200, and 1500 RPM. The nominal, upper limit, and lower limit vibration amplitudes are presented. Note that the effect of the uncertain scenario on the vibration amplitudes of the composite hollow shaft increase according to the rotation speed.

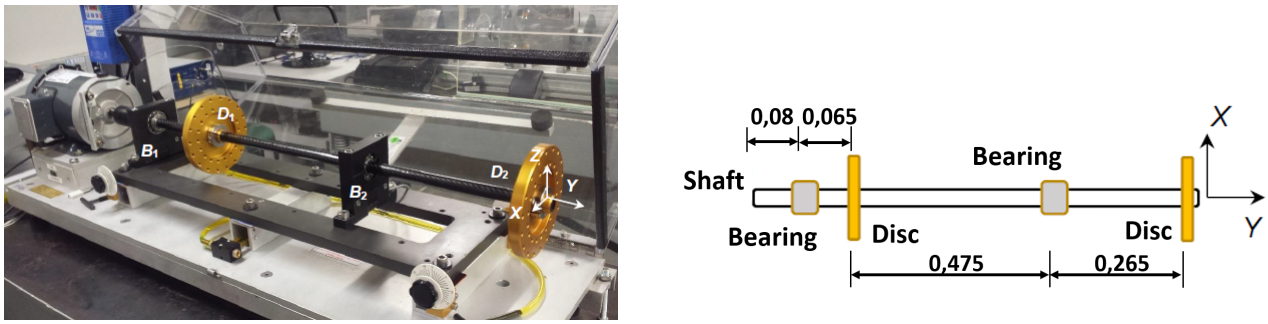

Figure 2. Experimental test rig.

Table 1. Uncertain intervals.

Parameters	Nominal values	$\mathbf{p_l}$	$\mathbf{p_u}$
Young's modulus at 0^o - E_1 (GPa)	103.67	98.49	108.86
Young's Modulus at $0^o/90^o$ - E_{12ext} (GPa)	127.05	120.70	133.41
Young's modulus at 90^o - E_2 (GPa)	47.50	45.12	49.87
Shear modulus - G_{12int} (GPa)	0.89	0.85	0.94
Shear modulus at $0^o/90^o$ - G_{12ext} (GPa)	3.05	2.90	3.20
Poisson's coefficient - υ_{12int}	0.31	0.28	0.32
Poisson's coefficient at $0^o/90^o$ - υ_{12ext}	0.28	0.26	0.29
Damping factor - ψ_{11}	2.67 x 10^{-7}	2.53 x 10^{-7}	2.80 x 10^{-7}
Damping factor - ψ_{12}	6.58 x 10^{-6}	6.25 x 10^{-6}	6.91 x 10^{-6}
Position of the bearing B1 - δl_{B1}(mm)	0	-1	1
Position of the disc D1 - δl_{D1}(mm)	0	-1	1
Position of the bearing B2 - δl_{B2}(mm)	0	-1	1
Position of the disc D2 - δl_{D2}(mm)	0	-1	1
Orientation of the fibers - $\delta\theta$(degrees)	0	-1	1

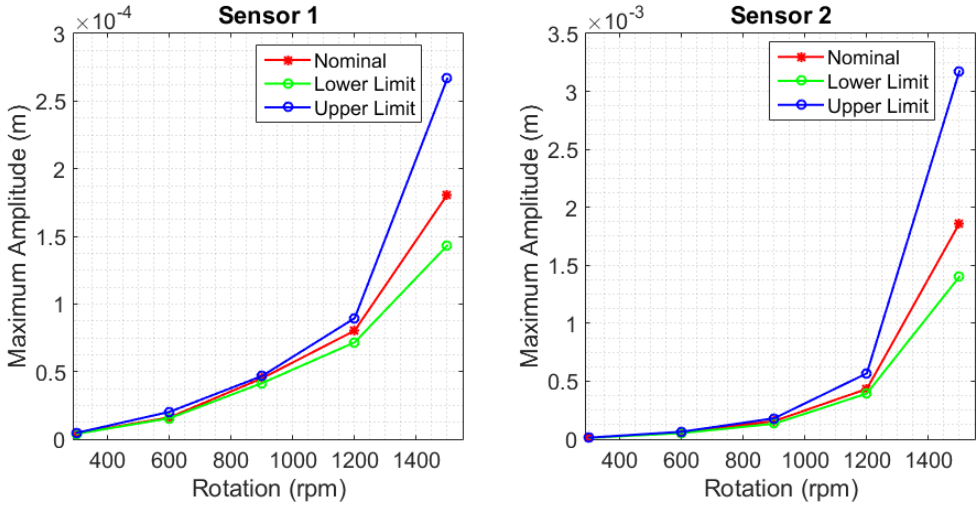

Figure 3. Uncertain envelopes.

Figures (4), (5) and (6) present the sensitivity analysis associated with the uncertain parameters of Tab. (1) for different rotation speeds (between 300 to 1500 RPM). The normalized relative sensitivity indexes ($\nu^{\bar{y}}_{\bar{p}_i}$, for $i = 1, ..., 14$) previously presented in Eq. (16) are computed for each of the fourteen uncertain interval parameters showed in Tab. (1). In this case, the chosen objective function was the maximum vibration amplitude of the composite shaft. Note that the sensitivity indexes for each uncertain parameter changed according to the rotation speed. For instance, it is possible to see in Fig. (4) that G_{12int} and G_{12ext} are very sensitive, presenting many peaks along the rotation speed range.

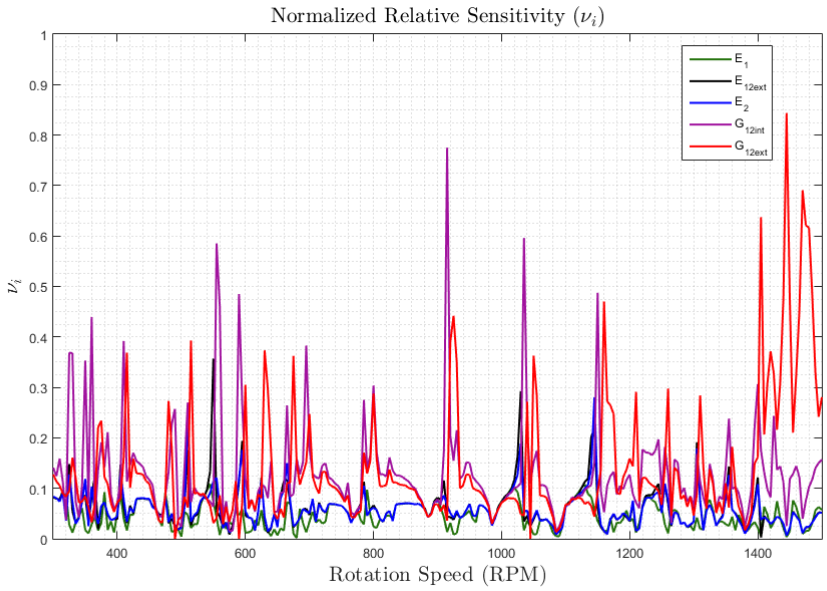

Figure 4. Normalized relative sensitivity indexes associated with the shaft parameters (Young's and shear moduli).

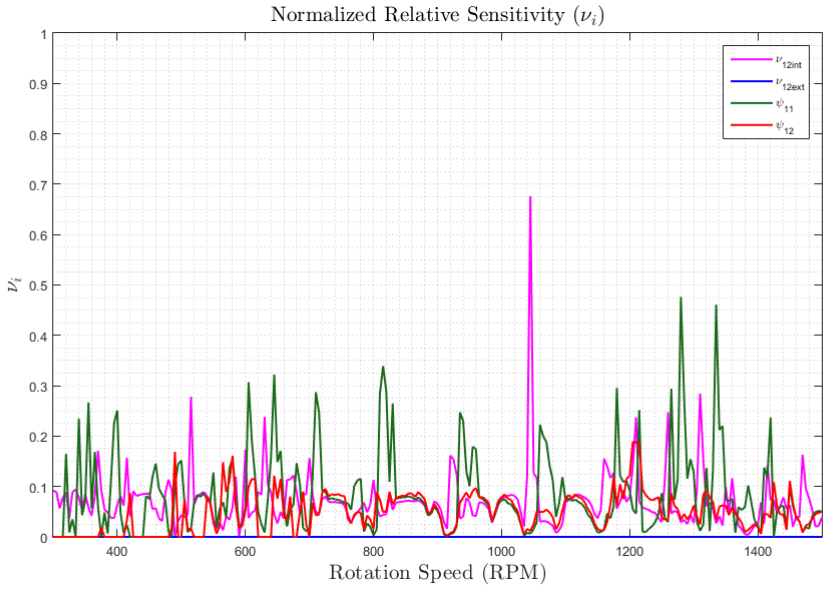

Figure 5. Normalized relative sensitivity indexes associated with the shaft parameters.

7. CONCLUSION

In the present contribution, an uncertainty analysis based on the interval approach was applied to a composite hollow shaft. A sensitivity analysis was also performed to evaluate the effects of the uncertain parameters on the dynamic behavior of the shaft. The SHBT method associated with the Timoshenko beam theory was used to obtain the FE model of the composite shaft. The obtained results demonstrated that the maximum vibration amplitude of the rotor is affected by the considered uncertain scenario, which increases according to the rotation speed of the rotor. Additionally, it was revealed that the sensitivity indexes of the considered uncertain parameters changed according to the rotation speeds. Thus, the obtained results demonstrated that the sensitivity analysis of the parameters of the composite shaft must be applied by considering the different rotation speeds of the system under its operating conditions.

8. ACKNOWLEDGEMENTS

The authors are thankful for the financial support provided to the present research effort by CNPq (574001/2008-5, 304546/2018-8, and 431337/2018-7), FAPEMIG (TEC-APQ-3076-09, TEC-APQ-02284-15, TEC-APQ-00464-16, and

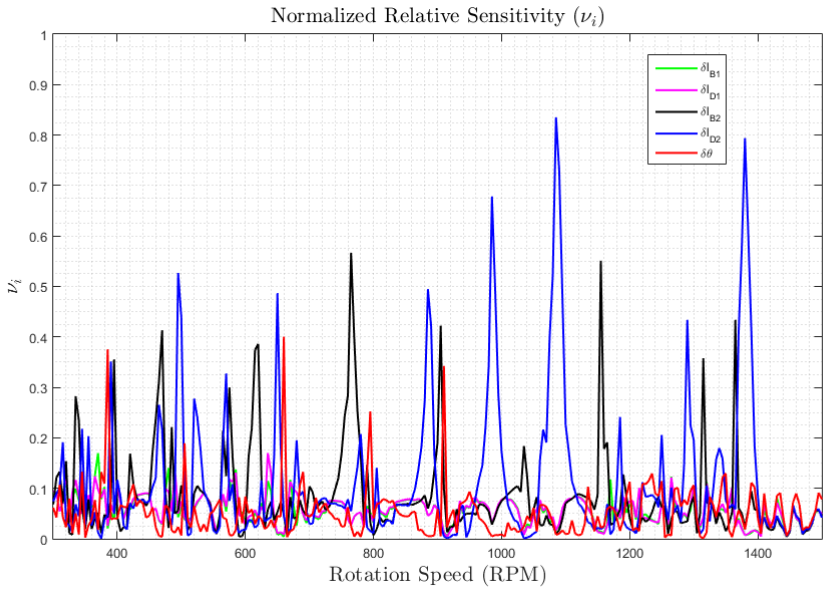

Figure 6. Normalized relative sensitivity indexes associated with the positions of the bearings, discs, and orientation of the fibers.

PPM-00187-18), and CAPES through the INCT-EIE.

9. REFERENCES

Brush, M., 1999. "Still spinning after all these years: A profile of the ultracentrifuge". *The Scientist*, Vol. 13, No. 20, pp. 16–18.

Cavalini Jr., A., Guimarães, T. and Steffen Jr., V., 2016. "Optimal design of a rotating machine containing a composite material shaft." *Brazilian Conference on Composite Materials*.

Gupta, K., 2015. "Composite shaft rotor dynamics: An overview". In *Vibration Engineering and Technology of Machinery*, Springer, pp. 79–94.

Koroishi, E.H., Lara-Molina, F.A. and Repinaldo, J.P., 2018. "Sensitivity analysis of smart rotor under to uncertainties". In *MATEC Web of Conferences*. EDP Sciences, Vol. 211, p. 18001.

Kuschmierz, R., Filippatos, A., Günther, P., Langkamp, A., Hufenbach, W., Czarske, J. and Fischer, A., 2015. "In-process, non-destructive, dynamic testing of high-speed polymer composite rotors". *Mechanical Systems and Signal Processing*, Vol. 54, pp. 325–335.

Lees, A.W., 2011. "Smart machines with flexible rotors". *Mechanical Systems and Signal Processing*, Vol. 25, No. 1, pp. 373–382.

Modares, M. and Mullen, R.L., 2013. "Dynamic analysis of structures with interval uncertainty". *Journal of Engineering Mechanics*, Vol. 140, No. 4, p. 04013011.

Moens, D. and Vandepitte, D., 2006. "Interval sensitivity analysis of dynamic response envelopes for uncertain mechanical structures". In *III European Conference on Computational Mechanics*. Springer, pp. 385–385.

Moens, D. and Vandepitte, D., 2007. "Interval sensitivity theory and its application to frequency response envelope analysis of uncertain structures". *Computer methods in applied mechanics and engineering*, Vol. 196, No. 21-24, pp. 2486–2496.

Molina, F.A.L., AP Cavalini JR, A., Koroishi, E.H. and Steffen Jr, V., 2019. "Sensitivity analysis of flexible rotor subjected to interval uncertainties".

Moore, R.E., Kearfott, R.B. and Cloud, M.J., 2009. *Introduction to interval analysis*, Vol. 110. Siam.

Sino, R., 2007. *Comportement dynamique et stabilité des rotors: application aux rotors composites*. Ph.D. thesis, Lyon, INSA.

Storn, R. and Price, K., 1997. "Differential evolution–a simple and efficient heuristic for global optimization over continuous spaces". *Journal of global optimization*, Vol. 11, No. 4, pp. 341–359.